Excited State Intramolecular Proton Transfer (ESIPT) from Phenol to Carbon in Selected Phenylnaphthols and Naphthylphenols

ARTICLE *in* THE JOURNAL OF ORGANIC CHEMISTRY · SEPTEMBER 2012

Impact Factor: 4.72 · DOI: 10.1021/jo301456y · Source: PubMed

7 AUTHORS, INCLUDING:

Jakov Ivkovic
Graz University of Technology
5 PUBLICATIONS **61** CITATIONS

SEE PROFILE

Lily Wang
University of Victoria
11 PUBLICATIONS **57** CITATIONS

SEE PROFILE

JOC The Journal of Organic Chemistry

Article

pubs.acs.org/joc

Excited State Intramolecular Proton Transfer (ESIPT) from Phenol to Carbon in Selected Phenylnaphthols and Naphthylphenols

Nikola Basarić,*[,†] Nađa Došlić,[‡] Jakov Ivković,[†] Yu-Hsuan Wang,[§] Jelena Veljković,[†] Kata Mlinarić-Majerski,[†] and Peter Wan[§]

[†]Department of Organic Chemistry and Biochemistry, Ruđer Bošković Institute, Bijenička cesta 54, 10000 Zagreb, Croatia

[‡]Department of Physical Chemistry, Ruđer Bošković Institute, Bijenička cesta 54, 10000 Zagreb, Croatia

[§]Department of Chemistry, University of Victoria, Box 3065 Stn CSC, Victoria BC, V8W 3 V6, Canada

Supporting Information

ABSTRACT: ESIPT and solvent-assisted ESPT in isomeric phenyl naphthols and naphthyl phenols **5**−**8** were investigated by preparative photolyses in CH_3CN−D_2O, fluorescence spectroscopy, LFP, and *ab initio* calculations. ESIPT takes place only in **5** (D-exchange Φ = 0.3), whereas **6**−**8** undergo solvent-assisted PT with much lower efficiencies. The efficiency of the ESIPT and solvent-assisted PT is mainly determined by different populations of the reactive conformers in the ground state and the NEER principle. The D-exchange experiments and calculations using RI-CC2/cc-pVDZ show that **5** in S_1 deactivates by direct ESIPT from the OH to the naphthalene position 1 through a conical intersection with S_0, delivering QM **14** that was detected by LFP (τ = 26 ± 3 ns). ESIPT to position 3 in **5** is possible but it proceeds from a less-populated conformer and involves an energy barrier on S_1. In solvent-assisted PT to naphthalene position 4 in **5**, zwitterion **17** is formed, which cyclizes to stable naphthofuran photoproducts **9**−**12**. The regiochemistry of the deuteration in solvent-assisted PT was correlated with the NBO charges of the corresponding phenolates/naphtholates **5**$^-$−**8**$^-$. Combined experimental and theoretical data indicate that solvent-assisted PT takes place *via* a sequential mechanism involving first deprotonation of the phenol/naphthol, followed by the protonation by H_2O in the S_1 state of phenolate/naphtholate. The site of protonation by H_2O is mostly at the naphthalene α-position.

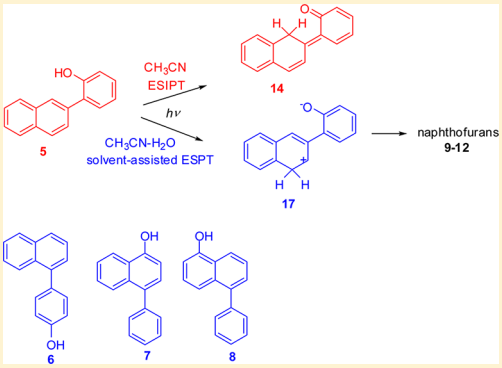

INTRODUCTION

Proton transfer in both ground and excited states is a fundamental process in chemistry and biology.[1] Upon electronic excitation, some organic functional groups exhibit enhanced acidity or basicity.[2] If these sites are in close proximity, upon electronic excitation an excited-state intramolecular proton transfer (ESIPT) can occur.[3] ESIPT has been the focus of intensive research because of its fundamental nature[2,3] as well as its many potential applications.[4] According to Kasha, ESIPT occurs *via* several reaction mechanisms including intrinsic intramolecular proton transfer (the true ESIPT), concerted biprotonic transfer, proton-relay tautomerization, and catalysis of proton transfer.[5] Whereas direct ESIPT has found applications in the synthesis of chromanes,[6] sensing,[7] laser dyes,[8] photostabilizers,[9] scintillators,[10] long-lived pH jumps,[11] or the photoswitching of polymorphs,[12] the proton-relay mechanism is particularly interesting in biological systems. Biological proton transfer generally takes place over long distances that may involve chains of polar amino acids and H_2O molecules.[13] Furthermore, light-initiated long-range proton transfer takes place in bacteriorhodopsin, enabling the function of a proton pump that moves protons through membrane against the gradient.[14] The solvent-relay mechanism of ESIPT has also been thoroughly investigated for 7-azaindoles[15] and 7-hydroxyquinoline[16] and has been used for the probing of structural dynamics in proteins.[17]

The most common acidic group in the ESIPT reactions is the phenolic O**H**, whereas the basic site is usually a heteroatom such as carbonyl oxygen or nitrogen of a heterocycle.[2,3] Furthermore, some examples are known wherein the photoprotonation of a carbon competes with the protonation of heteroatoms.[18] However, ESIPT to carbon usually takes place with much lower quantum efficiency.[19] Consequently, proton transfer (PT) involving a carbon acid or base is often inadvertently overlooked as a possible excited-state pathway. Nevertheless, we have a continuing interest in the acid−base chemistry of excited states, with a particular effort directed at discovering new examples of carbon photoacids or photobases.[20] ESIPT from the phenol OH to carbon atoms is now recognized as a general reaction as many examples have been documented by us involving phenol adjacent to the following rings: phenyl,[21] naphthyl,[22] anthryl[23] terphenyl[24] or pyrenyl.[25]

Special Issue: Howard Zimmerman Memorial Issue

Received: July 14, 2012
Published: September 6, 2012

More recently we reported a very efficient ESIPT reaction in 2-phenyl-1-naphthol (**1**) that gives QM **2**, **4** and zwitterion **3** (eq 1).[26] Formation of QMs **2**−**4** was inferred due to

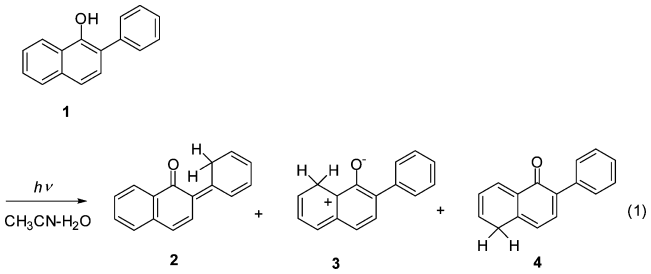

regiospecific incorporation of deuterium on irradiation in D_2O (D-exchange $\Phi = 0.7$), the highest efficiency ever reported for such a process. QM **2** was spectroscopically detected by laser flash photolysis (LFP) (τ = 20 ns). A theoretical investigation showed that ESIPT in aprotic solvents operates *via* a conical intersection with the ground state that represents the dominant deexcitation pathway from the singlet excited state surface. In water, a H_2O-mediated relay mechanism takes place *via* a conical intersection, delivering QMs and zwitterions.[26] The ESIPT in **1** was compared with the reaction in 2-phenylphenol. Due to the unfavorable conformer distribution in the S_0, ESIPT in 2-phenylphenol takes place with significantly lower efficiency (D-exchange $\Phi = 0.041$),[18,26] whereas ESIPT in the isomeric 1-phenyl-2-naphthol does not take place at all.[27]Herein, we describe a systematic study of ESIPT and solvent-assisted ESPT in a series of naphthalenes **5**−**8**. This series of compounds was designed to investigate the influence of the naphthalene vs naphthol chromophore on the efficiency and regioselectivity of ESIPT and solvent-assisted ESPT. Two compounds, **5** and **6**, have phenol as the acidic site attached to the naphthalene chromophore, whereas in **7** and **8** the phenyl is attached to the naphthol, which is the acidic site. Furthermore, naphthols **7** and **8** were chosen to investigate whether solvent-assisted PT can take place from the naphthol OH to the carbom atoms of the distal phenyl ring. Although not exhaustive, the available compounds shed new insights into the ESIPT process involving carbon bases. The compounds were investigated by irradiations in the presence of D_2O, fluorescence measurements and LFP. Rational explanations for the regioselectivity and efficiency of the PT processes were provided by high-level theoretical calculations.

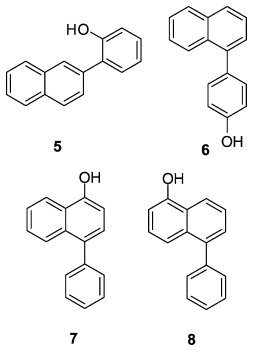

RESULTS AND DISCUSSION

Synthesis. Naphthalene derivatives **5**−**8** were prepared in high yields from the corresponding methoxy derivatives **5OMe**−**8OMe**, which were in turn synthesized by Suzuki coupling reactions (eqs 2 and 3).

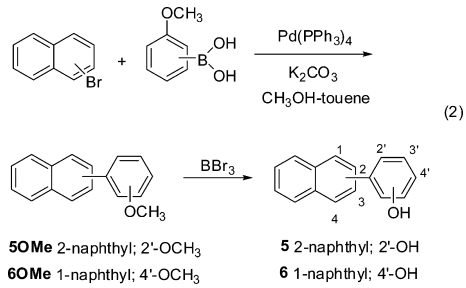

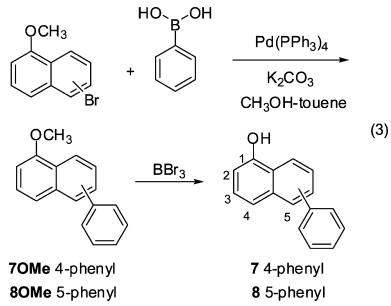

Photochemical Experiments. Irradiations of **5**−**8** were first performed in CH_3CN and CH_3CN−H_2O in UV−vis cuvettes to check for the formation of stable photoproducts. After each exposure to light, the UV−vis spectra were taken (see the Supporting Information). Irradiation of naphthols **7** and **8** in CH_3CN and CH_3CN−H_2O resulted in a broadening of the characteristic 1-naphthol absorption bands, suggesting formation of new products or decomposition of the samples (*vide infra*). Furthermore, irradiations of phenols **5** and **6** in CH_3CN did not change their UV−vis spectra, suggesting that these molecules in CH_3CN do not give stable photoproducts. However, on irradiation of **5** in CH_3CN−H_2O new structured bands at 350−400 nm appeared, clearly indicating formation of new products absorbing in that wavelength region.

To isolate stable photoproducts, preparative irradiations of **5**, **7** and **8** were performed in CH_3CN−H_2O and CH_3OH. Prolonged irradiations (1−4 h) of **7** and **8** gave only high molecular weight material and the starting material (which was recovered), indicating that the changes seen in the UV−vis spectra were due to decomposition. On the other hand, irradiation of **5** (1 h, 300 nm, 16 lamps) in CH_3CN−H_2O (3:1) resulted in conversion of 58% and gave four naphthofuran products **9**−**12** isolated in 3, 12, 15 and 6% yield, respectively (eq 4). Irradiation in CH_3OH (2 h) resulted in lower conversion of 48%, and gave products **9**, and **11**−**13** in 6, 16, 3 and 7% yield, respectively (eq 5). The structures of products **9** and **10** were determined by comparison of their 1D and 2D NMR spectra with those published in literature.[28,29] The structures of new naphthofuran derivatives **11**−**13** were determined with the help of 2D NMR techniques (COSY, NOESY, HSQC, HMBC, see the Experimental Section).

To probe for ESIPT involving C-atoms as a basic site, irradiations were performed in CH_3CN−D_2O mixtures, wherein incorporation of deuterium at carbon atoms denotes these pathways. Irradiations were typically performed in CH_3CN−D_2O (c(D2O) = 0.3 M) or CH_3CN−D_2O (2:1, $c(D_2O)$ = 14 M). After irradiations and aqueous workup the samples were analyzed by MS and NMR to determine the extent and position of deuteration, respectively. Irradiation (8 lamps, 300 nm, 1 h) of **1**, and **5**−**8** in CH_3CN−D_2O containing low concentration

dx.doi.org/10.1021/jo301456y | J. Org. Chem. 2013, 78, 1811−1823

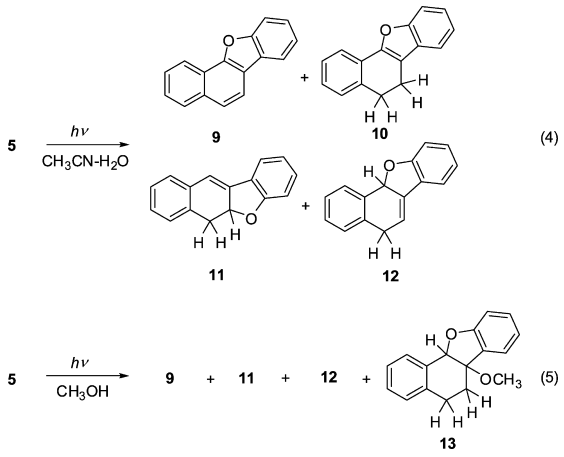

of D_2O (0.3 M) gave rise to deuterium incorporation only in **1** and **5**. Irradiation of **1** resulted in very efficient incorporation of D at the *ortho* position of the adjacent phenyl ring. After 1 h irradiation of **1**, both *ortho* H atoms were replaced by D.[26] Irradiation of **5** after 1 h gave quantitative exchange at the naphthalene position 1 (corresponding to **5-D1**) and 78% at the position 3 (**5-D3**), whereas MS indicated presence of 10% monodeuterad, 76% dideuterated, and 14% of trideuterated species. The observed incorporation of D is in accordance with ESIPT and formation of QMs that on subsequent thermal tautomerization give rise to deuterated starting molecules (*vide infra*). The other option for D-exchange would be efficient protonation of the naphthalene in the excited state by D_2O, as demonstrated by Shizuka et al. for methoxynaphthalenes.[30] However, since no D-exchange takes place on irradiation of methoxy derivatives **5OMe**−**8OMe**, this pathway probably does not take place or takes place with insignificant quantum efficiency.

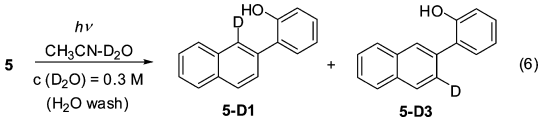

In a protic solvent, ESPT in 1-naphthol gives naphtholate (pK^*_a = 0.4).[31] In addition, solvent-assisted formal transfer of the OH proton to the distal carbon atom at the position 5 takes place with a quantum efficiency of 0.11, as evidenced by D-exchange experiments.[31,32] Photolyses of naphthols **1**, **7** and **8** and phenols **5** and **6** in CH_3CN-D_2O at $c(D_2O)$ = 14 M also gave rise to D-incorporation. Interestingly, the efficiency of the deuteration at lower D_2O concentration (c(D2O) = 0.3 M) for **1** and **5** was 10−20% higher than at $c(D_2O)$ = 14 M. The finding is in accordance with direct ESIPT mechanism of D-exchange in these derivatives that is partly perturbed on addition of more H_2O (D_2O). However, at higher D_2O concentration, in addition to direct ESIPT, solvent assisted ESPT gives rise to D-exchange at the distal positions.

Photolysis of **5** in CH_3CN-D_2O (2:1) gave rise to D-exchange in the molecule, and formation of deuterated products **9**-**12** (Scheme 1). To characterize all deuterated products preparative irradiation of **5** in CH_3CN-D_2O (3:1) was performed (100 mg, 2 h, 16 lamps, 300 nm). After chromatographic separation on TLC, 30% of **5-D** was isolated with D incorporated at C-1 (100%), C-3 (18%), C-4 (10%), C-6/7 (13%), and C-5/8 (100%). Naphthofuran **9-D** was isolated in 7% yield with D incorporated at C-10 (31%), C-3/4/6 (28%), and at C-5 (68%). Dihydronaphthalene derivative **10-D** was formed only in traces, isolated in a fraction enriched in **10-D**. NMR indicated that **10-D** contained one deuterium at C-6 and 85% D at C-5. In the aromatic part of the spectrum, due to overlapping of the signals, the position of the deuteration could not be determined. Naphthofuran derivatives **11-D** and **12-D** were isolated in 25% and 20% yield, respectively. **11-D** contained D at the naphthalene position 5 (15%), 6 (100%), 10 (30%), and 11 (74%), whereas **12-D** contained D at the naphthalene positions 5 (18%), 6 (100%), 8/9 (23%), 10 (47%), and 11 (83%). The irradiation experiment in CH_3CN-D_2O (3:1) was taken to higher conversion to isolate the deuterated products **9**−**12**. On the other hand, the irradiation taken to low conversions clearly indicate that **5D-1** is formed first, whereas formation of other derivatives takes place about 5−10 times slower.

Direct ESIPT in **6**−**8** is not possible due to a larger distance between the phenol ring and the proton-accepting rings. Therefore, a higher concentration of D_2O (protic solvent) is required to mediate the ESPT, which eventualy gives rise to deuteration at the distal sites. Irradiation (1 h) of **6** in CH_3CN-D_2O (2:1) resulted in D-incorporation at the naphthalene position 4 (10%, corresponding to **6-D4**, eq 7), and position 5/8 (45%).

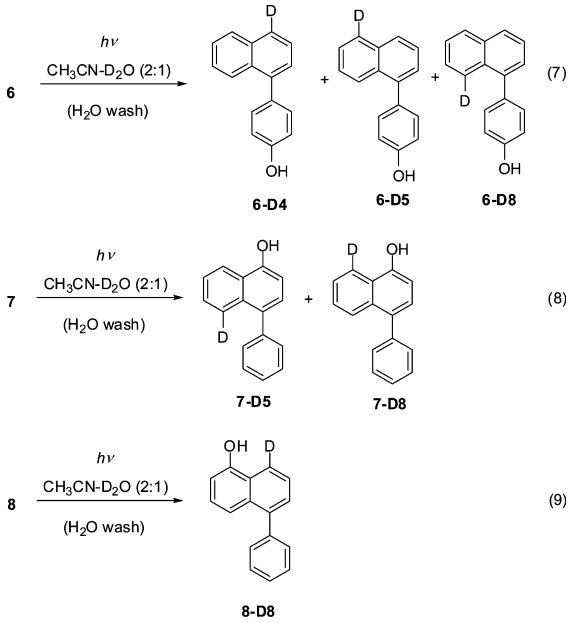

The MS analysis indicated presence of 34% of deuterated and 13% dideuterated species, and 3% trideuterated species. Irradiation of naphthol **7** gave rise to D-exchange at the positions 5 (16%) and 8 (11%), and MS indicated 30% of deuterated and 5% of dideuterated species (eq 8), whereas irradiation of **8** gave D only at the position 8 (15%), which was in agreement with the MS indicating 15% of deuterated species (eq 9).

Quantum yields of deuterium incorporation (see the Experimental Section) were determined by use of a secondary actinometer, D-exchange in 2-phenylphenol (Φ = 0.041),[21b] and a primary one, valerophenone (giving acetophenone in aqueous solvent Φ = 0.65).[33] Measurements were performed in triplicate and the mean value is reported (Table 1). Both actinometers gave similar values for the quantum yield of D-exchange, with the mean value within the error of the experiment. From the data it is clear that the quantum efficiency cannot be correlated with the direction of proton transfer, that is, excitation of phenol (**5** and **6**) vs. excitation of naphthol (**1**, **7**, **8**). In addition, the

dx.doi.org/10.1021/jo301456y | J. Org. Chem. 2013, 78, 1811−1823

Scheme 1. Main Products Obtained after Irradiation of 5 in CH_3CN-D_2O (3:1)[a]

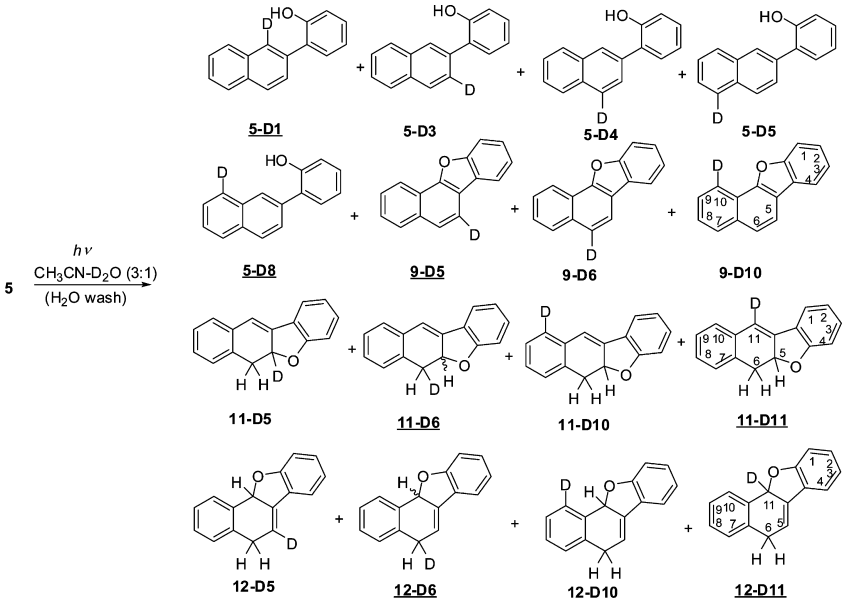

[a]Compounds with a high percentage of D (> 70%) are underlined.

Table 1. Quantum Yields for Deuterium Incorporation[a]

	Φ
1	0.73 ± 0.07[b]
5	0.30 ± 0.05
6	0.065 ± 0.005
7	0.02 ± 0.01
8	~0.01

[a]Photolysed in CH_3CN-D_2O (2:1) at 254 nm (2 lamps, Luzchem reactor). The actinometer was valerophenone in CH_3CN-H_2O (Φ = 0.65),[33] and D-exchange in 2-phenylphenol (Φ = 0.041).[21] [b]From ref 26.

efficiency of D-exchange is significantly higher for **1** and **5** wherein direct ESIPT along the H-bonding trajectory between the OH(OD) and the π-system is possible.

Fluorescence. Photophysical properties of the studied phenols and naphthols were characterized by UV−vis and fluorescence measurements. Fluorescence spectra (see the Supporting Information), quantum yields of fluorescence and singlet excited state lifetimes were measured in CH_3CN and CH_3CN-H_2O (1:4), wherein it was anticipated that the differences would arise due to solvent-assisted PT (Tables 2 and 3).

Table 2. Spectral Properties of 1, and 5−8

	λ_{max}/nm[a]	λ_{max}/nm[b]	$\Delta\upsilon_{ST}$/cm^{-1}[c]	$\Delta\upsilon_{HBW}$/cm^{-1}[d]	λ_{max}/nm[e]	ΔpK_a[f]
1	292	353.5/364	6774	3881	373 (~475)	
5	286	350.0	6394	3440	350 (518)	13.0
6	291	371.5	8166	4421	390 (518)	14.6
7	304	379.0	6509	4440	390 (454)	9.2
8	304	391.0	7319	4873	~400 (526)	11.4

[a]Maximum of the absorption spectrum in CH_3CN. [b]Maximum of the fluorescence spectrum in CH_3CN. [c]Stokes shift in CH_3CN. [d]Half-bandwidth of the fluorescence spectrum in CH_3CN. [e]Maximum of the fluorescence spectrum in CH_3CN-H_2O (1:4). The values in parentheses correspond to the emission from phenolate/naphtholate. [f]pK_a-pK_a* estimated by Förster cycle.

Table 3. Photophysical Properties of 1, and 5−8 in CH_3CN and CH_3CN-H_2O (1:4)

	Φ (CH_3CN)[a]	Φ (CH_3CN-H_2O)[a]	τ (CH_3CN)/ns[b]	τ (CH_3CN-H_2O)/ns[b]
1	0.031 ± 0.001[c]	0.032 ± 0.002[c]	0.3 ± 0.1 (30%)	3.0 ± 0.5 naphthol
			1.7 ± 0.1 (20%)	6.1 ± 0.5 naphtholate[c]
			10.0 ± 0.5 (50%)[c]	
5	0.04 ± 0.01	0.020 ± 0.002	1.3 ± 0.1	0.1 (1.8) phenol
6	0.19 ± 0.03	0.02 ± 0.001	0.64 ± 0.02	0.13 phenol
7	0.39 ± 0.08	0.25 ± 0.07	2.35 ± 0.01	1.6 (8.0) naphthol
				0.7 ± 0.1 naphtholate
8	0.44 ± 0.02	0.03 ± 0.01	2.5 ± 0.1 (88%)	
			4.07 ± 0.01 (12%)	4.9 ± 0.1 naphtholate

[a]Determined by use of quinine sulfate in 0.05 M aqueous H_2SO_4 (Φ = 0.53) or fluorene in CH_3OH (Φ = 0.68) as ref 36. [b]Measured by time-correlated single photon timing (SPT) method. [c]From ref 26.

UV−vis spectra of **1**, **7** and **8** are characterized by the presence of a broad absorption band, typical for α-naphthols, that gives rise to ^1L_a and ^1L_b states.[34] Naphthylphenol derivatives **5** and **6** absorb at slightly shorter wavelength, corresponding to the typical naphthalene absorption. The lowest excited state of **1** in CH_3CN can be characterized as ^1L_a.[35] Broader fluorescence spectra of **7** and **8** suggest the presence of two emissive states. Since **7** and **8** cannot have conformers with different photophysical properties, we attribute the finding to ^1L_a and ^1L_b states. A larger Stokes shift for **8** (compared to **1** and **7**) is probably due to a better charge delocalization with the phenyl at the naphthol position 5. In addition, the Stokes shift and the half-bandwidth is larger for **6** than for **5**, suggesting a higher charge-transfer character in the S_1 in **6**.

Fluorescence quantum yields for **1** and **5** in CH_3CN (Table 3) are 5−10 times lower than for **6**−**8**. The finding can be

dx.doi.org/10.1021/jo301456y | J. Org. Chem. 2013, 78, 1811−1823

rationalized by operation of efficient ESIPT in **1** and **5**, which lowers Φ_f, and is not possible in aprotic solvent for **6**–**8**. Fluorescence decays measured by time-correlated single photon timing (SPT) were single-exponential for CH_3CN solutions of **5**–**7**, giving singlet-excited state lifetimes (Table 3). On the contrary, fluorescence decays for **1** and **8** were fitted to three-, and two-exponential function, respectively, probably due to the presence of several emissive states.

Addition of H_2O to the CH_3CN solution of phenols and naphthols results in fluorescence quenching due to an opening of a new excited-state relaxation pathway, PT to solvent.[37] To probe for the influence of a protic solvent on the photophysical properties of **5**–**8**, fluorescence titrations with H_2O were performed (see the Supporting Information). However, addition of a small amount of H_2O (up to 2 M) to the CH_3CN solution of **5** increased fluorescence, suggesting that H_2O partly blocks the nonradiative deactivation pathway, ESIPT to carbon at the naphthalene position 1 (*vide supra*). A similar behavior was found for **1** and rationalized by efficient intrinsic ESIPT pathway giving rise to QM **2** that is partly quenched on addition of a protic solvent.[26] Further addition of H_2O (above 2.5 M) to the CH_3CN solution of **5** quenches fluorescence and changes the appearance of the fluorescence spectra. A new band appears at a longer wavelength that is seen only in the protic solvent and assigned to the fluorescence of phenolate formed by adiabatic PT to solvent. Adiabatic PT to aqueous solvent is also corroborated by SPT measurements. Single-exponential fluorescence decay in CH_3CN solution becomes two-exponential in CH_3CN–H_2O (1:4). The decay component contributing more at the shorter wavelengths can be assigned to phenol emission, whereas at longer wavelengths, the component with a negative pre-exponential factor that dominates corresponds to the phenolate emission.

Addition of H_2O to the CH_3CN solutions of **6**–**8** clearly resulted in fluorescence quenching, particularly for **6** and **8** wherein Φ_f in CH_3CN–H_2O (1:4) is more than 10 times lower than in neat CH_3CN. Furthermore, addition of H_2O gave rise to dual fluorescence due to adiabatic formation of fluorescent phenolate $\mathbf{6}^-$ and naphtholates $\mathbf{7}^-$ and $\mathbf{8}^-$ (Figure 1). Stronger

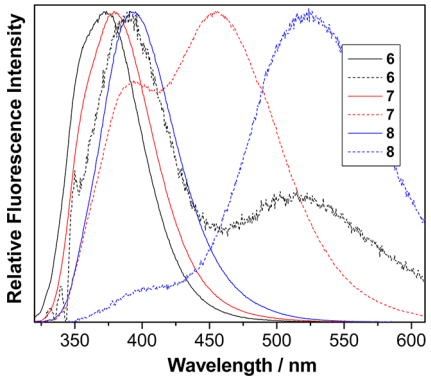

Figure 1. Normalized fluorescence spectra of **6**–**8** in CH_3CN (full) and CH_3CN–H_2O (1:4, dash).

fluorescence quenching for **8**, compared to **7**, is in line with higher increase in acidity in S_1, probably due to a larger charge-transfer character of the S_1 state in **8**. The steady state absorption and fluorescence spectra in neutral and basic solution enable approximation of the difference in the pK_a values between the S_1 and S_0 by use of the Förster cycle. The values of ΔpK_a for **5**–**8** are compiled in Table 2. The data strongly suggests that **6** and **8** are much stronger photoacids than **7**. However, Förster cycle analysis must be taken with some caution, as a more precise estimation of pK_a^* requires intrinsic rate constants of proton transfer.

Laser Flash Photolysis (LFP). LFP was performed to probe for QMs that are formed by ESIPT or solvent-assisted PT. The transient spectra were recorded in N_2- and O_2-purged CH_3CN and CH_3CN–H_2O solutions (see the Supporting Information). LFP of N_2-purged solution CH_3CN of **5** gave rise to a strong transient absorption with a maximum at 400 nm and absorbing into the visible region. The transient decayed with $k = (2.3 \pm 0.5) \times 10^5\ s^{-1}$ ($\tau = 4 \pm 1\ \mu s$), and was strongly quenched by O_2 (O_2-purged CH_3CN solution $k = (2.8 \pm 0.2) \times 10^7\ s^{-1}$, $\tau = 37 \pm 2$ ns). Based on literature precedent[38] and the observed quenching by O_2, the transient was assigned to the phenol triplet–triplet absorption. In O_2-purged solution, in addition to the triplet, a very-short-lived transient was detected (Figure 2)

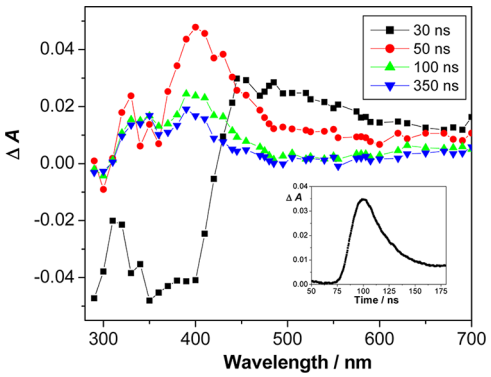

Figure 2. Transient absorption spectra of **5** in O_2-purged CH_3CN solution. Inset: decay at 500 nm.

absorbing at 400–600 nm decaying with $k = (4.0 \pm 0.4) \times 10^7\ s^{-1}$, $\tau = 26 \pm 3$ ns). Similarly to the transients observed by LFP of **1**,[26] the short-lived species could tentatively be assigned to QM **14**. In the transient spectra of **5** taken in CH_3CN–H_2O solution, due to a strong signal of the fluorescence stretching over the whole visible region, the short-lived transient was not observed. To verify if the observed short-lived transient corresponds to QM, LFP of **5OMe** (that cannot give QMs) was also undertaken. However, in the LFP spectra of **5OMe** taken in N_2-purged CH_3CN solution, we detected a signal corresponding to the triplet at 430 nm ($\tau \approx 3\ \mu s$) and transient absorption at $\lambda > 500$ nm that was not affected by O_2 (in O_2-purged CH_3CN, $k \approx 2 \times 10^5\ s^{-1}$, $\tau \approx 5\ \mu s$), probably corresponding to radical-cations formed by two photon ionization. Therefore, we cannot give a firm assignment of the short-lived transient observed by LFP of **5**, since it may correspond to radical-cation undergoing a very fast deprotonation.

LFP of CH_3CN or CH_3CN–H_2O solution of **6** gave rise to a strong transient absorption at 500 nm $k = (2–5) \times 10^5\ s^{-1}$ ($\tau = 2–5\ \mu s$), that was quenched by O_2, which we have assigned to the triplet state. In addition, in CH_3CN–H_2O, a more persistent transient was detected at 430 nm (O_2 purged solution $k = (2.1 \pm 0.1) \times 10^4\ s^{-1}$, $\tau = 45 \pm 2\ \mu s$. In comparison with published spectra,[38] the transient was assigned to the phenoxyl radical, probably formed by two photon ionization, initially giving a phenol radical-cation and solvated electron. Radical-cations deprotonate readily in protic solvent, giving phenoxyl radicals. Therefore, we observed a stronger transient absorption

dx.doi.org/10.1021/jo301456y | J. Org. Chem. 2013, 78, 1811–1823

corresponding to phenoxyl radicals in aqueous solution. LFP of naphthol **8** also gave rise to a signal corresponding to the triplet absorbing with a maximum at 480 nm (in N_2-purged CH_3CN, $k = (1.35 \pm 0.05) \times 10^6$ s^{-1}, $\tau = 730 \pm 30$ ns), and a more persistant transient, probably corresponding to phenoxyl radicals. The longer-lived transient for **7** absorbed at $\lambda = 325$ nm, 400 nm, and had a shoulder at 500 nm, stretching over the visible region, decayed with $k = (2.5 \pm 0.5) \times 10^4$ s^{-1}, ($\tau = 40 \pm 10$ μs). Similarly, the phenoxyl radical was detected in the LFP of **8** that in CH_3CN–H_2O had a maximum at 350 nm and a shoulder at 400 nm decaying with $k \approx 2 \times 10^4$ s^{-1}, $\tau \approx 50$ μs.

Quantum Chemical Calculations. Additional insight into the photochemistry of the investigated phenylnaphthols and naphthylphenols is provided by *ab initio* calculations. Specifically, the calculations were aimed to rationalize the outcome of the D-exchange experiments. Ground-state geometries of several low energy conformers of **5**–**8** were obtained by employing the MP2/TZVP method in the gas phase and in the framework of the polarizable continuum model MP2/PCM/TZVP (Table 4). With respect to the orientation of the OH group and the adjacent proton accepting ring, we distinguish between the *syn* (**S**) and *anti* (**A**) conformers.

Table 4. Electronic Energies of Several Low Energy Conformers of 5–8 Computed at the MP2/TZVP and MP2/PCM/TZVP Levels[a]

	MP2/TZVP	MP2/PCM/TZVP
S1	0.00	0.00
A1	3.79	2.63
S5–1	0.00	0.00
S5–3	0.23	0.25
A5–1	2.72	1.29
A5–3	1.80	1.28
S6	0.00	0.04
A6	0.09	0.00
A7	0.00	0.00
S7	2.33	2.34
A8	0.00	0.00
S8	2.32	2.32

[a]The energies are given in kcal/mol relative to the corresponding minimum energy conformer.

The quantum yields of deuterium incorporation are strongly affected by the ground state population equilibrium of the *syn* and *anti* conformers. MP2/PCM/TZVP yields four minimum energy structures of **5**. The two lowest energy structures correspond to the *syn* conformers **S5–1** and **S5–3**. These structures favor direct ESIPT to the naphthalene position 1 and 3. The **A5–1** and **A5–3** forms are found 1.29 and 1.28 kcal/mol higher in energy, respectively, resulting in a Boltzmann population ratio of 0.54:0.34:0.06:0.06 for **S5–1**:**S5–3**:**A5–1**:**A5–3**. Contrary to **5**, the energetics of **6** is not sensitive to the orientation of the OH group. However, the large separation between the OH and the naphthalene ring makes the direct ESIPT impossible. On the other hand, in **7** and **8** direct ESIPT is in principle conceivable. However, in the low energy structures **A7** and **A8**, the OH group is directed away from the second naphthol ring. The *syn* oriented conformers **S7** and **S8** are found to be more than 2.3 kcal/mol higher in energy. That is, in **7** and **8**, the ground state conformational equilibrium effectively precludes direct ESIPT to the naphthalene position 8. The obsereved differences in the photochemical reactivity therefore can be explained by the NEER principle (nonequilibration of the excited-state rotamers).[39]

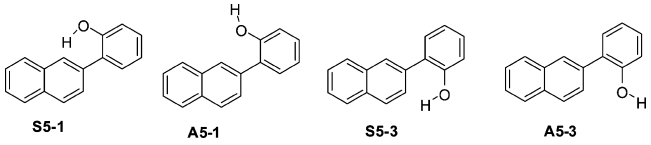

Vertical electronic excitations for **5**–**8** were computed using RI-CC2/cc-pVDZ. Energies for the first two excited states of **5**–**8** are compiled in Table 5. The results correspond to the gas phase excitation and are directly comparable with the experimental results for **5**. However, for **6**–**8**, larger deviations between the experimental values obtained in CH_3CN solution (Table 2) and the calculated results were obtained.

Table 5. Vertical and Adiabatic Excitations (nm) for 5–8 Computed using RI-CC2/cc-pVDZ[a]

state	S5–1	S5–3	S6	A7	A8
S_1	285 ($CI_{S1/S0}$)	284 (334)	280 (308)	285 (340)	284 (347)
S_2	268	262	265	273	274

[a]The value in parentheses corresponds to adiabatic excitation energy.

The leading excitations contributing to the S_1 state of **S5–1** are of $\pi\pi^*$ type with charge transfer (CT) character (Figure 3).

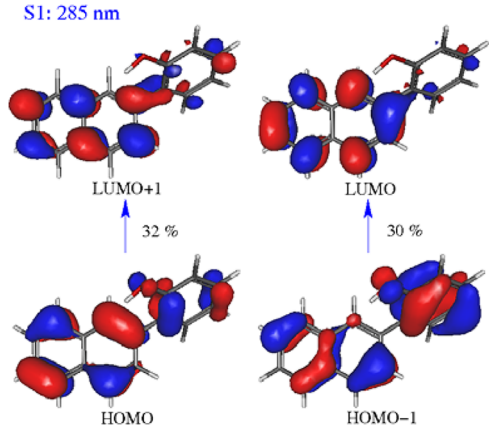

Figure 3. Occupied (bottom) and unoccupied (top) molecular orbitals of the S_1 state of **S5–1** at the geometry of vertical excitation.

The occupied orbitals are delocalized on both rings while the unoccupied ones are localized on the naphthyl ring. This is in contrast to **1**, where the occupied orbitals are localized on the naphthol ring and the unoccupied one is completely delocalized. However, the net effect is the same—an effective transfer of negative charge from one ring, here the phenol, to the other. This is evident from Figure 4 where the difference in the electron densities between the S_1 and S_0 is shown. Note also the strong redistribution of charge within the naphthyl ring. The leading excitations contributing to the S_1 state of **6** and **8** are shown in the Supporting Information.

The geometry optimization of the S_1 state in **S5–1** leads to the stretching of the OH bond, rotation of the phenol ring with concomitant reduction of the torsional angle between the two rings from 57.3 to 37.5 degrees, and finally to ESIPT to the position 1 of the naphthyl ring. These geometrical changes greatly destabilize S_0 and the two states intersect 2.46 eV above the S_0 minimum. The optimization of **S5–3** in the S_1 state does

dx.doi.org/10.1021/jo301456y | J. Org. Chem. 2013, 78, 1811–1823

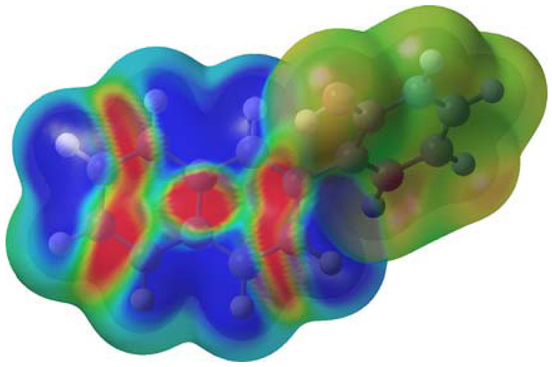

Figure 4. Difference in the electronic densities of **5** between states S_1 and S_0 evaluated at the electron density surface of S_0 with isovalue of 0.01/ Å^3. The areas of increased electron density are shown in blue.

not lead to CI with S_0 and hence to direct ESIPT. Instead, a minimum energy structure is found 0.48 eV (11.1 kcal/mol) below the S_1 vertical excitation. However, the barrier encountered on the ESIPT pathway is very small, less than 0.1 eV. The difference in energy between the vertical and adiabatic excitation corresponds to the gain in kinetic energy at the S_1 minimum. This energy gain is clearly larger than the barrier to ESIPT and ensures formation of QM **15**. In a protic solvent, the redistribution of the excess kinetic energy into atomic motion probably gives rise to the deprotonation and formation of naphthyl-phenolate **5**$^-$−**3**$^-$.

For **6**−**8**, direct ESIPT is not possible. Furthermore, Table 5 reveals that minima are located on the S_1 surfaces of the major conformers **S6**, **A7**, and **A8**. On the basis of the large difference between the vertical and adiabatic transitions we expect, however, that in the presence of proton-accepting solvent, adiabatic deprotonation takes place. The anions **5**$^-$−**8**$^-$ have been optimized at the same RI-CC2/cc-pVDZ level of theory and the natural bond orbital (NBO) analysis has been performed on all the minima. The adiabatic excitation energies of **5**−**1**$^-$, **6**$^-$, **7**$^-$, **8**$^-$, are 552 nm, 663 nm, 463 and 661 nm, respectively. Table 6 lists the NBO charges on the carbon atoms. We expect that the carbon atoms bearing the most negative charge are the preferred sites of deuterium incorporation in a $H_2O(D_2O)$-mediated reaction.

Table 6. NBO Charges on C-atoms in the Optimized S_1 State of the Anions (Phenolates and Naphtholates)[a]

C-atom	**5**−**1**$^-$	**6**$^-$	**7**$^-$	**8**$^-$
1	−0.25392	−0.19462	0.40255	0.38543
2	−0.15077	−0.24956	−0.22240	−0.21576
3	−0.23718	−0.27601	−0.27088	−0.29003
4	**-0.29656**	**-0.30096**	**0.03196**	**-0.10835**
5	**-0.30199**	**-0.29935**	**-0.39492**	**-0.08504**
6	−0.28021	−0.27478	−0.27554	−0.28490
7	−0.25980	−0.25927	−0.24021	−0.19643
8	**-0.29796**	**-0.32651**	**-0.34349**	**-0.31488**
9	−0.05505	−0.02381	−0.11546	−0.09540
10	−0.03596	−0.04712	−0.08275	−0.09619
1′	0.02595	0.08277	−0.05848	−0.10233
2′	0.32677	−0.23697	−0.22287	−0.25461
3′	−0.23773	−0.22307	−0.24372	−0.23494
4′	−0.27758	0.33621	−0.23428	−0.32406
5′	−0.17042	−0.22314	−0.24838	−0.23390
6′	−0.26999	−0.23085	−0.19466	−0.27045

[a]Notation of C-atoms follow IUPAC nomenclature rules and can be found in Scheme 2 and eqs 11, 12, and 13. C-atoms marked in bold are the preferred sites for D-incorporation.

The computed NBO charges on the oxygen atoms of **5**$^-$−**8**$^-$ are −0.435, −0.491, −0.559 and −0.602, respectively, and illustrate the proton affinity of the corresponding RO^- groups. Focusing on **5**$^-$, we see that apart from C-1, which is the target of direct ESIPT, carbon atoms C-4, C-5, and C-8 are prone to $H_2O(D_2O)$ attack. In **6**$^-$, the most probable sites of attack are again C-4, C-5, and C-8, while in **7**$^-$ these are C-5 and C-8, and in **8**$^-$ they are C-3 and C-8. Apart form **5**$^-$ where the NBO charge on oxygen is lower than (more negative), but to some extent comparable to, the most basic carbon atoms, in **6**$^-$−**8**$^-$ RO^- is the most probable site of $H_2O(D_2O)$ attack. These findings are in very good agreement with the observed regioselectivity and lower quantum yields of D-exchange (Table 1).

Photochemical Reaction Mechanisms. With the above experimental and theoretical results, photochemical reaction mechanisms for **5**−**8** can be proposed. Irradiation of **5** in aprotic solvent (or with low H_2O concentration) leads to an ultrafast efficient deactivation from the S_1 via a conical intersection with the S_0, delivering QM **14**, and less efficient deactiviation, also via a conical section delivering QM **15** (eq 10).

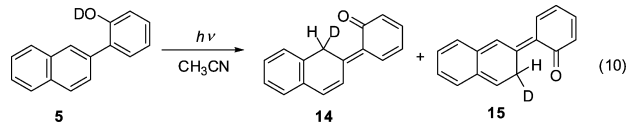

According to the D-exchange experiments, QMs **14** and **15** are formed in a ratio 5:1, which correlates with the relative energies of the reactive phenol conformations **S5**−**1** and **S5**−**3**. Due to efficient ESIPT delivering QMs **14** and **15**, fluorescence quantum yield of **5** in CH_3CN is low. Addition of protic solvent (H_2O) increases fluorescence due to a hindering of ESIPT, as seen for **1**.[26] However, at a high enough H_2O concentration, a new photochemical deacivation pathway from S_1 takes place involving deprotonation of the phenol OH. That is demonstrated in the fluorescence spectra where an additional band at longer wavelenghts can be observed, assigned to the fluorescence from phenolate formed in an adiabatic PT to solvent. Once phenolate in S_1 is populated, the anion undergoes protonation by H_2O at the distal sites, at C-4 and C-8, giving zwitterion **17** and QM **16** (Scheme 2). *Ab initio* calculation strongly indicates that protonation by H_2O takes place after deprotonation of the phenol since regioselectivity of the D-incorporation correlates with the calculated charges in the **5**−**1**$^-$ and not with the neutral **S5**−**3** in S_1. The signals in ^{1}H NMR corresponding to the H-atoms at C-5 and C-8 of the naphthalene overlap. Therefore, according to the NMR spectra after D-exchange, we cannot distinguish if photochemical reaction gives QM **16** or zwitterion **21**. However, **21** is probably not formed since we have not observed formation of products **22** and **23** that would arise from **21**.

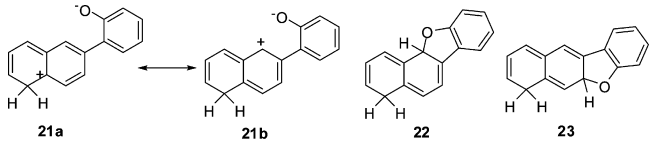

We have not detected H_2O-adducts **18**−**20** suggesting that QMs **14**−**16** do not react with H_2O (or CH_3OH) giving adducts (a known reaction for QMs), or that **18**−**20** are not stable products. Probably, QMs **14**−**16** only undergo tautomerization

dx.doi.org/10.1021/jo301456y | J. Org. Chem. 2013, 78, 1811−1823

Scheme 2

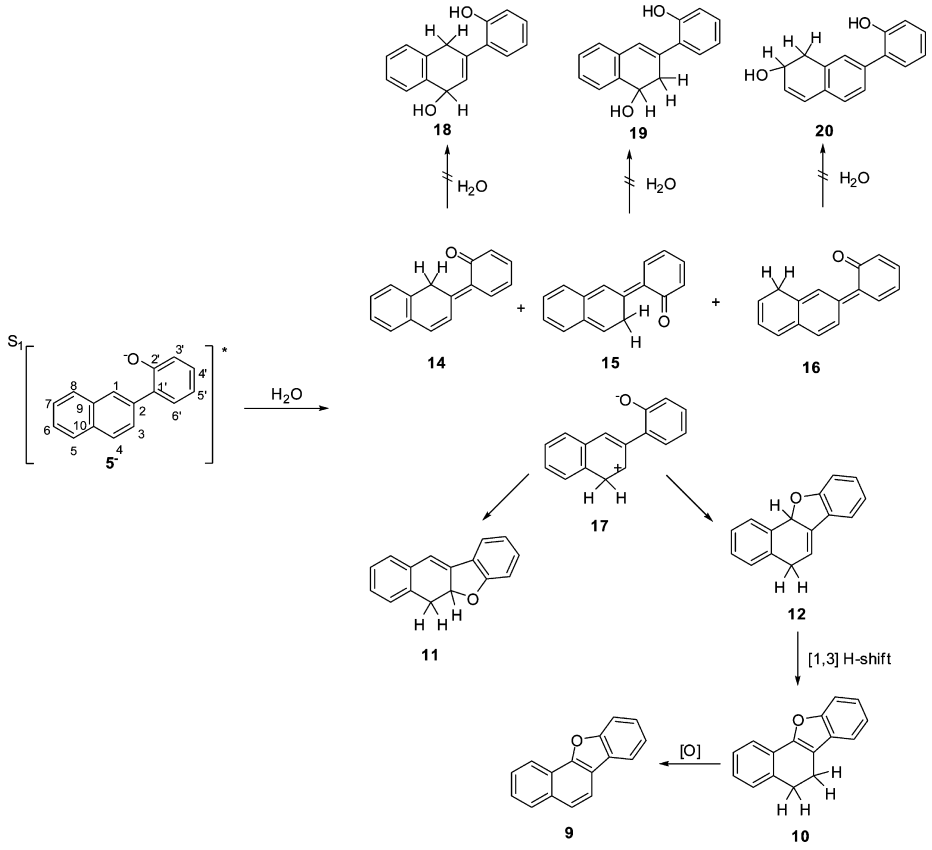

to the starting material. However, we cannot firmly rule out a pathway involving formation of **18**–**20** followed by a rapid elimination of H_2O. On irradiation in the presence of D_2O, deuterated QMs are formed that tautomerize to **5**. However, due to the primary isotope effect, D favorably remains regioselectively incorporated in the molecule. Contrary to **14**–**16** which only tautomerize to **5**, zwitterion **17** cyclizes to stable photoproducts **11** and **12**. Furthermore, naphthofuran **12** undergoes thermal or photochemical secondary [1,3] H-shift yielding **10**, whereas naphthofuran **9** is probably formed from **10** by aromatization due to the trace-impurities of O_2. After irradiation of **5** in CH_3CN–D_2O only a small content of D is found in the position 4 of the naphthalene. The finding indicates that **17** undergoes faster cyclization to **11** and **12** than tautomerization to the starting material.

After irradiation in CH_3CN–D_2O, **10**–**12** were isolated with D-incorporated in the molecules (Scheme 1). As indicated by D-exchange experiments taken to lower conversions, the fastest process is formation of **5D-1**. That is, the quantum yield for ESIPT in **5** giving **14** is about ten times higher than solvent-assisted PT giving **17**. Therefore, the isolated product **11** contained a high percentage of D at the position 11. Furthermore, afer the first fast D-exchange at the naphthalene position 1, deuterated **5**–**1D** undergoes second photochemical reaction wherein D enters at the naphthalene position 4 and gives QM **17** that irreversibly cyclize to **11**. Consequently, isolated **11** contained a high percentage of dideuterated species, wherein one D was quantitatively incorporated at the position 6 and the other was at a high percentage at the position 11 (corresponding to **11-D6** and **11-D11**). Similarly, after irradiation in CH_3CN–D_2O, product **12** was isolated with one deuterium quantitatively incorporated at the position 6, and some molecules contained 2 deuteriums, at positions 6 and 11.

Compounds **6**–**8** are photochemicaly stable in CH_3CN since transfer of the OH proton from the naphthalene or phenol OH to the distal carbon sites cannot take place without protic solvent. Therefore, all of **6**–**8** are characterized by high fluorescence quantum yields in neat CH_3CN, almost an order of magnitude higher than for **1** and **5**. Excitation of **6**–**8** to S_1 results in an increase of dipole moment in these molecules. The difference in the calculated and measured absorption is probably due to a neglect of the stabilization by solvent in the calculations. Stronger polarization of the molecules in S_1 leads to enhanced acidity of the phenol or naphthol OH. Therefore, excitation to S_1 in a protic solvent gives rise to deprotonation and formation of phenolates/naphtholates, along with fluorescence quantum yields significantly lower than in neat CH_3CN. After deprotonation, the naphtholates or phenolates in S_1 undergo protonation by H_2O (D_2O) that give QMs. Phenolate $\mathbf{6}^-$ is protonated at the naphthalene positions 4, 5, and 8, yielding QMs **24**–**26** (eq 11). The regioselectivity of D-exchange is correlated with the calculated negative charge in S_1 of the phenolate. Similarly, in protic solvent, naphthols **7** and **8** in S_1 deprotonate giving naphtholates. Due to a better charge stabilization with the phenyl at position 5, **8** is more acidic than **7**, which is corroborated by fluorescence measurements. Subsequent protonation of the naphtholate $\mathbf{7}^-$ and $\mathbf{8}^-$ gives QMs **27** and **28**, or **29**, respectively (eqs 12 and 13). Due to significantly lower quantum efficiency for the solvent-assisted PT than for the direct ESIPT, QMs in the photochemical reactions of **6**–**8** are formed less efficiently than from **1** and **5**. Hence, we were not able to detect **24**–**29** by LFP.

dx.doi.org/10.1021/jo301456y | J. Org. Chem. 2013, 78, 1811–1823

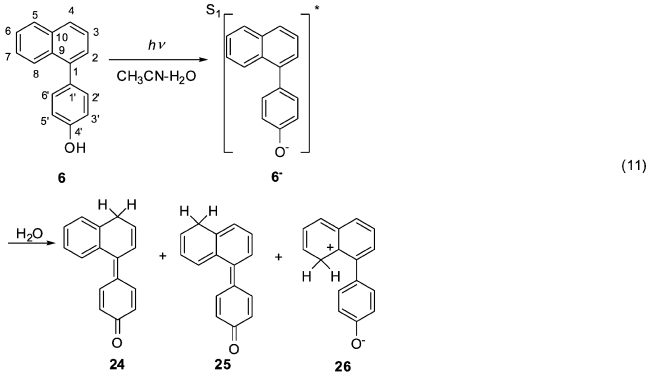

(11)

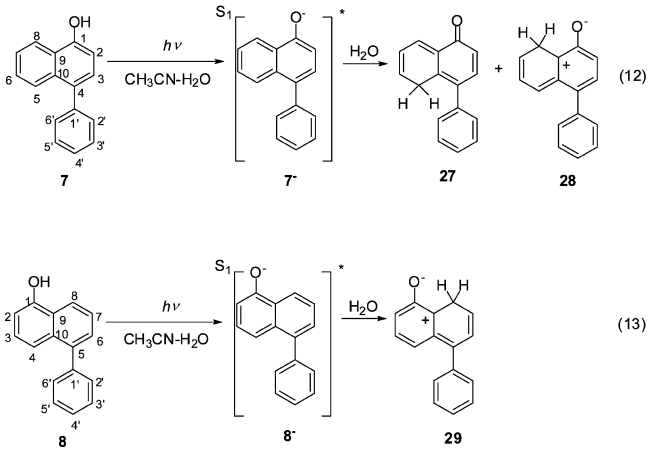

(12)

(13)

CONCLUSIONS

Phenols **5** and **6** and naphthols **7** and **8** undergo ESIPT or solvent-assisted PT from the phenol/naphthol OH to the carbon atoms of the adjecent aromatic ring giving quinone methide intermediates. In addition, solvent-assisted PT in **5** gives zwitterions that undergo cyclization to naphthofurans **9**−**12**. Investigation of the photophysical properties and photoreactivity of **5**−**8** reveal significantly higher photochemical reactivity in systems where direct ESIPT is possible. Solvent-assisted PT takes place with quantum yields that are 5−10 times lower. The probable mechanism for solvent-assisted PT involves first the deprotonation of the OH group in the S_1 state, followed by protonation by H_2O of carbon atoms of the naphtholate/phenolate on the same surface. Furthemore, photochemical reactivity is highly correlated with the conformational distribution in the ground state representing another example of the operation of the NEER principle.

EXPERIMENTAL SECTION

General. ^1H and ^{13}C NMR spectra were recorded on 300, 500, or 600 MHz. The NMR spectra were taken in $CDCl_3$ or DMSO-d_6 at rt using TMS as a reference and chemical shifts were reported in ppm. For the assignment of signals, 2D homonuclear COSY and NOESY and heteronuclear HSQC and HMBC techniques were used. Melting points were determined using a Mikroheiztisch apparatus (and were not corrected). UV−vis spectra were recorded on a spectrophotometer at rt. IR spectra were recorded on a spectrophotometer in KBr. Deuterium content was determined by MS recorded on an instrument by use of the electrospray ionization technique. The spectra were obtained in the negative mode in the presence of triethylamine. Accurate mass determination was performed on an ESI-quadrupole instrument. A mg/mL solution of the analyte was diluted by a factor of 10−100 and injected by liquid infusion at ∼300−500 nL/min by syringe pump through a nano ESI source; all solvents used were MS grade. For the sample analysis, a HPLC equipped with a Diode-Array detector and a C18(2) column was used. Mobile phase was CH_3OH−H_2O (20%). For the chromatographic separations, silica gel (0.05−0.2 mm) was used. Analytical thin layer chromatography was performed on SILG/UV_{254} plates. Irradiation experiments were performed in a reactor equipped with 2, 8, or 16 lamps with the output at 254 or 300 nm. During irradiations in the reactor, the irradiated solutions were continuously purged with Ar and cooled by a tap water finger condenser. Solvents for irradiations were of HPLC purity. Chemicals (bromonaphthalenes, boronic acids, solution of BBr_3) were purchased from the usual commercial sources or prepared according to the known procedures. Solvents for chromatographic separations were purified by distillation.

Suzuki Reaction, General Procedure. A two neck flask (100 mL) equipped with a condenser and a nitrogen inlet was charged with a methanol solution (15 mL) of boronic acid (10 mmol) and a toluene solution (35 mL) of bromonaphthalene (10 mmol). To the mixture was added anhydrous potassium carbonate (2.73 g, 19.72 mmol) and *tetrakis*-triphenylphosphine palladium $Pd(PPh_3)_4$ (0.17 g, 0.148 mmol), and the mixture was heated at the temperature of reflux for 24 h. The next day, to the cooled mixture H_2O (50 mL) was added and the layers were separated. The aqueous layer was extracted with CH_2Cl_2 (3 × 30 mL); the organic layers were combined and dried over anhydrous $MgSO_4$. After filtration, the solvent was removed on a rotary evaporator to afford crude product that was purified on a column of silica gel using hexane−CH_2Cl_2 (3:1) as eluent.

2-(2-Methoxyphenyl)naphthalene (5OMe).[40] From 2-methoxyphenyl boronic acid (1.5 g, 10 mmol) and 2-bromonaphthalene (2.07 g, 10 mmol), in the presence of potassium carbonate (2.76 g, 20 mmol) and $Pd(PPh_3)_4$ (0.17 g, 0.15 mmol), the reaction furnished 1.92 g (83%) of the product in the form of colorless crystals.

1-(4-Methoxyphenyl)naphthalene (6OMe).[41] From 4-methoxyphenyl boronic acid (1.0 g, 6.6 mmol) and 1-bromonaphthalene (0.91 mL, 6.6 mmol), in the presence of potassium carbonate (1.82 g, 13.2 mmol) and $Pd(PPh_3)_4$ (0.11 g, 0.1 mmol), the reaction furnished 1.11 g (72%) of the product in the form of colorless crystals.

1-Methoxy-4-phenylnaphthalene (7OMe).[42] From phenyl boronic acid (0.77 g, 6.6 mmol) and 1-bromo-4-methoxynaphthalene (0.91 mL, 6.6 mmol), in the presence of potassium carbonate (1.75 g, 12.6 mmol) and $Pd(PPh_3)_4$ (0.11 g, 0.1 mmol), the reaction furnished 0.51 g (34%) of the product in the form of colorless crystals.

1-Methoxy-5-phenylnaphthalene (8OMe).[43] From phenyl boronic acid (0.44 g, 3.6 mmol) and 1-bromo-5-methoxynaphthalene (0.80 g, 3.4 mmol), in the presence of potassium carbonate (0.94 g, 6.8 mmol) and $Pd(PPh_3)_4$ (60 mg, 0.05 mmol), the reaction furnished 610 mg (76%) of the product in the form of colorless crystals.

General Procedure for the Removal of the Methyl Ether Groups from Phenols with BBr_3. Reaction was carried out under N_2-atmosphere in a three-neck round-bottom flask (250 mL) equipped with a septum and a syringe. In the flask was placed methoxy derivative **5OMe**−**8OMe** (10 mmol), dissolved in dry CH_2Cl_2 (100 mL) and the solution was cooled to 0 °C by ice bath. To the cold solution, a solution of BBr_3 in CH_2Cl_2 (1 M, 30 mL) was added dropwise by use of a syringe during 1 h. After the addition was completed, the stirring was continued for 1 h at 0 °C and then at rt overnight. The next day, H_2O (100 mL) was added to the reaction mixture, the layers were separated, and the aqueous layer was extracted with CH_2Cl_2 (3 × 50 mL). The combined organic extracts were dried over anhydrous $MgSO_4$, solid was removed by filtration, and solvent was removed on a rotary evaporator. The obtained crude product was purified on a column filled with silica gel by use of CH_2Cl_2 and CH_2Cl_2−EtOAc (4:1) as eluent or crystallization.

2-(2-Hydroxyphenyl)naphthalene (5).[44] From 2-(2-methoxyphenyl)naphthalene (**5OMe**, 1.64 g, 7.0 mmol) and solution of BBr_3 (1M, 20 mL), the reaction gave 1.54 g of the crude product that was purified by chromatography on silica gel by use of CH_2Cl_2

dx.doi.org/10.1021/jo301456y | J. Org. Chem. 2013, 78, 1811−1823

and CH_3OH (1 → 3%) as eluent to afford 1.22 g (80%) of the pure product in the form of colorless crystals.

1-(4-Hydroxyphenyl)naphthalene (6).[45] From 1-(4-methoxyphenyl)naphthalene (**6OMe**, 0.81 g, 3.4 mmol) and solution of BBr_3 (1M, 10 mL), the reaction gave the crude product that was purified by chromatography on silica gel by use of CH_2Cl_2 and CH_2Cl_2−EtOAc (4:1) as eluent to afford 0.74 g (99%) of the pure product in a form of colorless crystals.

4-Phenyl-1-naphthol (7).[46] From 1-methoxy-4-phenylnaphthalene (**7OMe**, 0.25 g, 1.1 mmol) and solution of BBr_3 (1M, 3.2 mL), the reaction gave the crude product that was purified by chromatography on silica gel by use of CH_2Cl_2 and CH_2Cl_2−EtOAc (4:1) as eluent to afford 220 mg (91%) of the pure product in a form of colorless crystals.

5-Phenyl-1-naphthol (8).[47] From 1-methoxy-5-phenylnaphthalene (**8OMe**, 0.51 g, 2.2 mmol) and solution of BBr_3 (1M, 6.5 mL), the reaction gave the crude product that was purified by chromatography on silica gel by use of CH_2Cl_2 and (1 → 3%) CH_3OH as eluent to afford 436 mg (90%) of the pure product in a form of colorless crystals.

Irradiation of 2-(2-Hydroxyphenyl)naphthalene (5). A solution of **5** (100 mg, mmol) in CH_3CN−H_2O (3:1, 100 mL) was poured in a quartz vessel, purged with Ar for 30 min, and irradiated 1 h in a reactor (16 lamps, 300 nm). After the irradiation, extraction with CH_2Cl_2 was carried out (3 × 50 mL). The extracts were dried over anhydrous $MgSO_4$ and filtered and the solvent was removed on a rotary evaporator. The crude residue was chromatographed on a thin layer of silica using CH_2Cl_2/hexane (1:3) as eluent, to afford pure photoproducts and regenerate 42 mg (42%) of the starting material.

Benzo[*d*]naphtho[1,2-*b*]furan (9).[28] Three milligrams (3%); colorless crystals, ^{1}HNMR ($CDCl_3$, 500 MHz) δ/ppm 8.44 (d, 1H, J = 8.1 Hz, H-10), 7.96−8.02 (m, 3H, H-4, H-6), 7.77 (d, 1H, J = 8.2 Hz, H-5), 7.70 (d, 1H, J = 8.0 Hz, H-1), 7.63 (dd (t), 1H J = 7.4 Hz, H-9), 7.55 (dd, 1H, J = 7.5 Hz, J = 7.0 Hz, H-8), 7.47 (dd, 1H, J = 7.5 Hz, J = 8.1 Hz, H-2), 7.38 (dd (t), 1H, J = 7.5 Hz, H-3); ^{13}C NMR ($CDCl_3$, 125 MHz) δ/ppm 155.9 (s), 151.9 (s), 133.0 (s), 128.4 (d, C-7), 126.4 (d, C-9), 126.1 (d, C-2), 126.0 (d, C-8), 125.0 (s), 123.2 (d, C-5), 122.8 (d, C-3), 121.3 (s), 120.8 (d), 120.2 (d), 119.1 (s), 118.4 (d, C-6), 111.7 (d, C-1).

5,6-Dihydrobenzo[*d*]naphtho[1,2-*b*]furan (10).[29] Twelve milligrams (12%); colorless crystals, ^{1}HNMR ($CDCl_3$, 500 MHz) δ/ppm 7.65 (d, 1H, J = 7.5 Hz, H-10), 7.50 (d, 1H, J = 8.2 Hz, H-1), 7.49 (d, 1H, J = 7.5 Hz, H-4), 7.18−7.30 (m, 5H), 3.09 (t, 2H, J = 8.0 Hz, H-6), 2.95 (t, 2H, J = 8.0 Hz, H-5); ^{13}C NMR ($CDCl_3$, 125 MHz) δ/ppm 155.2 (s), 151.7 (s), 135.8 (s), 128.2 (s), 127.9 (d), 127.7 (s), 127.5 (d), 126.7 (d), 123.9 (d), 122.6 (d), 120.4 (d, C-10), 119.0 (d, C-4), 114.0 (s, C-4a), 111.3 (d, C-1), 28.6 (t, C-6), 19.2 (t, C-5).

5a,6-Dihydrobenzo[*d*]naphtho[2,3-*b*]furan (11). Fifteen milligrams (15%); colorless crystals, mp 123−125 °C; ^{1}HNMR ($CDCl_3$, 500 MHz) δ/ppm 7.48 (d, 1H, J = 7.5 Hz, H-1), 7.22−7.26 (m, 3H, H-3, H-9, H-7), 7.18 (d, 1H, J = 7.0 Hz, H-10), 7.14 (dd (t), 1H, J = 7.4 Hz, H-8), 6.96 (dd (t), 1H, J = 7.6 Hz, H-2), 6.93 (d, 1H, J = 8.2 Hz, H-4), 6.62 (d, 1H, J = 3.1 Hz, H-11), 5.27 (ddd, 1H, J = 3.1 Hz, J = 7.1 Hz, J = 15.8 Hz, H-5), 3.27 (dd, 1H, J = 7.1 Hz, J = 14.3 Hz, H-6), 3.12 (dd (t), 1H, J = 15.0 Hz, H-6); ^{13}C NMR ($CDCl_3$, 125 MHz) δ/ppm 164.2 (s, C−O1), 140.2 (s, C-1b), 135.0 (s, C-6a), 131.2 (s, C-10a), 130.4 (d, C-3), 128.9 (d, C-7), 127.4 (d, C-9), 126.8 (d, C-8/10), 126.7 (d, C-8/10), 124.5 (s, C-1a), 121.5 (d, C-1), 121.2 (d, C-2), 113.9 (d, C-11), 110.7 (d, C-4), 82.3 (d, C-5), 34.2 (t, C-6); HRMS (ESI) calculated for $C_{16}H_{12}O$ (+H^+) 221.0961, found 221.0966.

HMBC interactions: H-6 and C-5, C-1b, C-6a, C-10a, C-7, H-5 and C-11, C-1b, C-6 and H-7, H-11 and C-5, C-1a, C-10, H-1 and C-11, C−O1, C-1b, C-3, H-4 and C−O1, C-1, C-1a, H-2 and C-4, C-1a, H-10 and C-11, H-8 and C-7, C-10a.

5,11a-Dihydrobenzo[*d*]naphtho[1,2-*b*]furan (12). Six milligrams (6%); yellow crystals; mp 92−95 °C; ^{1}HNMR ($CDCl_3$, 500 MHz) δ/ppm 7.67 (d, 1H, J = 7.5 Hz, H-10), 7.41 (d, 1H, J = 7.5 Hz, H-4), 7.28−7.33 (m, 2H, H-8, H-9), 7.25 (d, 1H, J = 7.2 Hz, H-7), 7.19 (dd (t), 1H, J = 7.7 Hz, H-2), 6.96 (d, 1H, J = 8.0 Hz, H-1), 6.91 (dd (t), 1H, J = 7.5 Hz, H-3), 6.28 (dd, 1H, J = 2.5 Hz, J = 6.3 Hz, H-5), 5.78 (dd, 1H, J = 2.5 Hz, J = 8.7 Hz, H-11), 3.60 (ddd, 1H, J = 2.1 Hz, J = 6.3 Hz, J = 19.4 Hz, H-6), 3.37 (dd, 1H, J = 8.7 Hz, J = 19.4 Hz, H-6); ^{13}C NMR ($CDCl_3$, 125 MHz) δ/ppm 162.5 (s, C−O1), 139.4 (s, C-4b), 135.8 (s, C-10a), 133.2 (s, C-6a), 129.7 (d, C-2), 127.3 (d, C-8/9), 127.0 (d, C-7), 126.2 (d, C-8/9), 124.8 (s, C-4a), 124.5 (d, C-10), 121.0 (d, 2C, C-3, C-4), 113.0 (d, C-5), 110.6 (d, C-1), 81.1 (d, C-11), 31.7 (t, C-6); HRMS (ESI) calculated for $C_{16}H_{12}O$ (+Na^+) 243.0780, found 243.0780.

HMBC interactions: H-6 and C-5, C-4b, C-10a, C-6a, C-8, H-11 and C-10a, H-5 and C-6, C-4a, C-6a, C-6 and H-5, H-8/9, C-11 and H-10, H-8/9, H-1 and C-3/4, C-4a, C−O1, H-3 and C-1, C-3/4, C-4a, C-2, H-2 and C-3/4, C−O1, H-7 and C-10, C-6a, H-8/9 and C-10a.

General Irradiation in CH_3CN−D_2O. To a solution of naphthalene derivative (5 mg, 0.023 mmol) in CH_3CN (38 mL) was added D_2O (12 mL). The solution was purged with Ar for 30 min and irradiated in a reactor at 254 or 300 nm (16 lamps) for 1 or 10 min. After irradiation, 50 mL of H_2O was added and extractions with CH_2Cl_2 (3 × 50 mL) were carried out. The extracts were dried over anhydrous $MgSO_4$. After filtration and evaporation of the solvent, crude mixture was analyzed by NMR and MS.

Alternatively, naphthalene derivative (10 mg, 0.046 mmol) was dissolved in CH_3CN (10 mL). The solution was divided into two parts and poured into two quartz cuvettes. To the first cuvette CH_3CN (5 mL) and D_2O (100 μL) were added, and to the second CH_3CN (5 mL) and D_2O (5 mL). Both solutions were purged with Ar (30 min), sealed and irradiated at the same time in a reactor equipped with a merry-go-round using 8 lamps with the output at 300 nm for 1 h. To the irradiated solutions H_2O (20 mL) was added and extractions with CH_2Cl_2 (3 × 30 mL) were carried out. The extracts were dried over anhydrous $MgSO_4$. After filtration and evaporation of the solvent, crude mixture was analyzed by NMR and MS.

Control experiments were performed by preparing the same solution as described above that were kept in dark and worked-up with H_2O. After extractions with CH_2Cl_2 drying over anhydrous $MgSO_4$, filtration and evaporation of the solvent, the mixture was analyzed by NMR and MS.

Irradiation of 5 in CH_3CN−D_2O. To a solution of **5** (100 mg, 0.45 mmol) in CH_3CN (80 mL) was added D_2O (20 mL). The solution was purged with Ar for 30 min and irradiated in a reactor at 300 nm (16 lamps) for 2 h. After the irradiation, 50 mL of H_2O was added and extractions with CH_2Cl_2 (3 × 50 mL) were carried out. The extracts were dried over anhydrous $MgSO_4$, the solution was filtered and the solvent removed on a rotary evaporator. The residue was chromatographed on a thin layer of silica gel using CH_2Cl_2/hexane (1:3) as eluent.

9-D 7 mg (7%) 31% D at C-10, 28% D at C-3/4/6, 68% D at C-5.

10-D traces (<1%) 1D at C-6 and 85% D at C-5.

11-D 25 mg (25%) 30% D at C-10, 74% D at C-11, 15% D at C-5, 1D (108%) at C-6; MS (ESI): 17% 1D, 27% 2D, 18% 3D, 18% 4D.

12-D 20 mg (20%) 47% D at C-10, 23%D at C-8/9, 18% D at C-5, 83%D at C-11, 1D (110%) at C-6; MS (ESI): 16% 1D, 27% 2D, 23% 3D, 13% 4D, 7% 5D.

5-D 30 mg (30%) 10%D at C-4, 1D at C-1, 1D (107%) at C-5/8, 18% D at C-3, 13% D at C-6/7; MS (ESI): 13% 1D, 32% 2D, 25% 3D, 10% 4D.

Irradiation of 5 in CH_3OH. A solution of **5** (110 mg, 0.5 mmol) in CH_3OH (100 mL) was purged with Ar for 30 min and irradiated in a reactor at 300 nm (16 lamps) for 1 h. After the irradiation, the solvent was removed on a rotary evaporator. The residue was chromatographed on a thin layer of silica gel using CH_2Cl_2/hexane (1:5) and hexane/EtOAc (4:1) as eluent to afford **9** (7 mg, 6%), **11** (18 mg, 16%), **12** (3 mg, 3%), **13** (8 mg, 7%), and **5** (68 mg, 62%).

6a-Methoxy-5,6,6a,11a-tetrahydrobenzo[*d*]naphtho[1,2-*b*]furan (13). Colorless oil; ^{1}HNMR ($CDCl_3$, 500 MHz) δ/ppm 7.52 (d, 1H, J = 7.5 Hz, H-10), 7.29 (dd, 1H, J = 1.0 Hz, J = 7.5 Hz, H-4), 7.26 (t, 1H, J = 7.5 Hz, H-9), 7.19−7.23 (m, 2H, H-8, H-2), 7.08 (d, 1H, J = 7.5 Hz, H-7), 6.95 (dt, 1H, J = 0.7 Hz, J = 7.5 Hz, H-3), 6.79 (d, 1H, J = 8.0 Hz, H-1), 5.60 (s, 1H, H-11), 3.15 (s, 3H, OCH_3), 2.70 (dd, 1H, J = 4.5 Hz, J = 15.7 Hz, H-6), 2.49 (ddd, 1H, J = 3.5 Hz, J = 11.8 Hz, J = 15.7 Hz, H-6), 2.39 (ddd, 1H, J = 3.5 Hz, J = 4.5 Hz,

dx.doi.org/10.1021/jo301456y | J. Org. Chem. 2013, 78, 1811−1823

J = 12.8 Hz, H-5), 2.19 (ddd, 1H, J = 4.5 Hz, J = 11.8 Hz, J = 12.8 Hz, H-5); ^{13}C NMR ($CDCl_3$, 125 MHz) δ/ppm 160.7 (s, C−O1), 138.1 (s, C-10a/6a), 134.0 (s, C-10a/6a), 130.5 (d, C-2), 130.3 (d, C-10), 128.2 (d, C-7), 127.9 (d, C-8), 126.7 (d, C-9), 125.9 (s, C-4a), 124.5 (d, C-4), 120.6 (d, C-3), 110.5 (d, C-1), 85.3 (s, C-4b), 85.2 (d, C-11), 50.7 (q), 32.8 (t, C-6), 26.9 (t, C-5); HRMS (ESI) calculated for $C_{17}H_{16}O_2$ (+Na^+) 275.1043, found 275.1050.

Quantum Yields for the D-Incorporation. Solutions of naphthalene derivatives **5**−**8** in CH_3CN−D_2O (3:1), as well as a solution of valerophenone in CH_3CN−H_2O (1:1) were freshly prepared and their concentrations were adjusted to have absorbances 0.4−0.8 at 254 nm. After adjustment of the concentration and measurement of the corresponding UV−vis spectra, the solutions were filled in quartz cuvettes (15 mL), purged with a stream of N_2 (20 min each), and sealed with a septum. The cuvettes were irradiated at the same time in a reactor equipped with a merry-go-round and 2 lamps with the output at 254 nm for 0.5, 1, and 2 min. After each irradiation, the samples were taken from the cuvettes by use of a syringe and analyzed by ESI MS (the D content was determined from the difference of the intensity of signals of irradiated and nonirradiated sample), whereas the conversion of valerophenone was analyzed by HPLC. Quantum yields for the D-exchange was calculated using valerophenone actinometer (formation of acetophenone in aqueous media, Φ = 0.65 ± 0.03).[33]

Alternatively, **5**−**8** (5 mg, 0.023 mmol) were dissolved in CH_3CN (32 mL). To the solution was added D_2O (12 mL). The solution was purged with Ar for 30 min and irradiated in a reactor at 254 (16 lamps) for 1 min. During irradiation, the solution was continuously purged with Ar and cooled by a coldfinger condenser. After irradiation, 50 mL of H_2O was added and extractions with CH_2Cl_2 (3 × 50 mL) were carried out. The extracts were dried over anhydrous $MgSO_4$. Under the same conditions, 2-phenylphenol (6 mg, 0.03 mmol), dissolved in CH_3CN−D_2O (3:1, 50 mL), was irradiated for 10 min. After aqueous workup, extraction and removal of the solvent, the extent of the deuterium incorporation was determined by ^{1}H NMR. Quantum yield for the D-exchange was calculated using D-exchange in 2-phenylphenol as a secondary actinometer (Φ = 0.041 ± 0.03).[21]

Steady State and Time-Resolved Fluorescence Measurements. The steady state measurements were performed on a luminescence spectrometer. The samples were dissolved in CH_3CN, or CH_3CN−H_2O (1:4) and the concentrations were adjusted to have absorbances at the excitation wavelength (270, 290, 300, or 310 nm) < 0.1. Solutions were purged with nitrogen for 30 min prior to analysis. The measurements were performed at 20 °C. Fluorescence quantum yields were determined by comparison of the integral of the emission bands with the one of fluorene in methanol (Φ = 0.68) or quinine sulfate in 0.05 M aqueous H_2SO_4 (Φ = 0.53).[36] The measurements were performed in triplicate and the mean value was reported. Typically, three absorption traces were recorded (and averaged) as well as three fluorescence emission traces, exciting at three different wavelengths. Three quantum yields were calculated and the mean value was reported.

Fluorescence decay histograms were obtained on an instrument equipped with a light emitting diode (excitation wavelength 265 or 310 nm), using time-correlated single photon counting technique in 1023 channels. Histograms of the instrument response functions (using LUDOX scatterer) and sample decays were recorded until they typically reached 3 × 10^3 counts in the peak channel. The half width of the instrument response function was typically ∼1.5 ns. The time increment per channel was 0.049 or 0.098 ns. Obtained histograms were fitted as sums of exponential using Gaussian-weighted nonlinear least-squares fitting based on Marquardt−Levenberg minimization implemented in the software package of the instrument. The fitting parameters (decay times and pre-exponential factors) were determined by minimizing the reduced chi-square χ^2. An additional graphical method was used to judge the quality of the fit that included plots of surfaces ("carpets") of the weighted residuals vs channel number.

Laser Flash Photolysis (LFP). All LFP studies were conducted employing a YAG laser, with a pulse width of 10 ns and excitation wavelength 266 nm. Static cells (0.7 cm) were used and solutions were purged with nitrogen or oxygen for 20 min prior to measurements. Absorbances at 266 nm were ∼0.4.

Computational Methods. The ground state equilibrium geometries of **5**−**8** have been determined with the second order Møller−Plesset (MP2) method and the triple-ζ valence plus polarization (TZVP) basis set.[48] Solvation effects were estimated with the polarizable continuum model (PCM)[49] using the dielectric constant of CH_3CN as implemented in the Gaussian09 program package.[50] The vertical excitation energies, optimized geometries, and ESIPT reaction paths have been determined with the second order approximate coupled cluster (CC2) method with the cc-pVDZ basis set.[51] The resolution of identity (RI) approximation has been used for the evaluation of the electron repulsion integrals.[52] All coupled cluster calculations and the natural bond orbital (NBO) analysis[53] have been performed with the TURBOMOLE package.[54]

■ ASSOCIATED CONTENT

Supporting Information

Copies of the ^{1}H and ^{13}C NMR spectra, UV−vis, fluorescence, LFP, and computational data. This material is available free of charge via the Internet at http://pubs.acs.org.

■ AUTHOR INFORMATION

Corresponding Author

*Fax: + 385 1 4680 195. Tel: +385 1 4561 141. E-mail: nbasaric@irb.hr.

Notes

The authors declare no competing financial interest.

■ ACKNOWLEDGMENTS

These materials are based on work financed by the Croatia Foundation for Science, Higher Education and Technological Development of the Republic of Croatia (HRZZ grant no. 02.05/25), the Ministry of Science Education and Sports of the Republic of Croatia (grants No. 098-0982933-2911 and 098-0352851-2921), the Natural Sciences and Engineering Research Council (NSERC) of Canada and the University of Victoria.

■ DEDICATION

This article is dedicated to the memory of Professor Howard E. Zimmerman.

■ REFERENCES

(1) *Hydrogen-transfer Reactions*; Hynes, J. T., Klinman, J. P., Limbach, H.-H., Schowen, R. L., Eds.; Wiley-VCH: Weinheim, 2007.

(2) (a) Ireland, J. F.; Wyatt, P. A. H. *Adv. Phys. Org. Chem.* **1976**, *12*, 131−221. (b) Arnaut, L. G.; Formosinho, S. J. *J. Photochem. Photobiol. A: Chem.* **1993**, *75*, 1−20.

(3) (a) Klöpffer, W. *Adv. Photochem.* **1977**, *10*, 311−358. (b) Formosinho, S. J.; Arnaut, L. G. *J. Photochem. Photobiol. A: Chem.* **1993**, *75*, 21−48. (c) Ormson, S. M.; Brown, R. G. *Prog. React. Kinet.* **1994**, *19*, 45−91. (d) Le Gourrierec, D.; Ormson, S. M.; Brown, R. G. *Prog. React. Kinet.* **1994**, *19*, 211−275.

(4) Kwon, J. I.; Park, S. Y. *Adv. Mater.* **2011**, *23*, 3615−3642.

(5) Kasha, M. *J. Chem. Soc., Faraday Trans. 2* **1986**, *82*, 2379−2392.

(6) Argumun, S.; Popik, V. V. *J. Am. Chem. Soc.* **2011**, *133*, 5573−5579.

(7) (a) Choi, K.; Hamilton, A. D. *Angew. Chem., Int. Ed.* **2001**, *40*, 3912−3915. (b) Klymchenko, A. S.; Demchenko, A. P. *J. Am. Chem. Soc.* **2002**, *124*, 12372−12379. (c) Peng, X.; Wu, Y.; Fan, J.; Tian, M.; Han, K. *J. Org. Chem.* **2005**, *70*, 10524−10531. (d) Batista, R. M. F.; Oliveira, E.; Costa, S. P. G.; Lodeiro, C.; Raposo, M. M. M. *Org. Lett.* **2007**, *9*, 3201−3204.

(8) (a) Parthenopoulos, D. A.; McMorrow, D. P.; Kasha, M. *J. Phys. Chem.* **1991**, *95*, 2668−2674. (b) Douhal, A.; Amat-Guerri, F.; Acuña, A. U.; Yoshihara, K. *Chem. Phys. Lett.* **1994**, *217*, 619−625. (c) Park,

S.; Kwon, O.-H.; Kim, S.; Park, S.; Choi, M.-G.; Cha, M.; Park, S. Y.; Jang, D.-J. *J. Am. Chem. Soc.* **2005**, *127*, 10070−10074.
(9) (a) Stueber, G. J.; Kieninger, M.; Schettler, H.; Busch, W.; Goeller, B.; Franke, J.; Kramer, H. E. A.; Hoier, H.; Henkel, S.; Fischer, P.; Port, H.; Hirsch, T.; Rytz, G.; Birbaum, J.-L. *J. Phys. Chem.* **1995**, *99*, 10097−10109. (b) Keck, J.; Kramer, H. E. A.; Port, H.; Hirsch, T.; Fischer, P.; Rytz, G. *J. Phys. Chem.* **1996**, *100*, 14468−14475.
(10) (a) Kauffman, J. M. *Radiat. Phys. Chem.* **1993**, *41*, 365−371. (b) Pla-Dalmau, A. *J. Org. Chem.* **1995**, *60*, 5468−5473.
(11) Nunes, R. M. D.; Pineiro, M.; Arnaut, L. G. *J. Am. Chem. Soc.* **2009**, *131*, 9456−9462.
(12) Mutai, T.; Tomoda, H.; Ohkawa, T.; Yabe, Y.; Araki, K. *Angew. Chem., Int. Ed.* **2008**, *47*, 9522−9524.
(13) (a) Lill, M. A.; Helms, V. *Proc. Natl. Acad. Sci. U.S.A.* **2002**, *99*, 2778−2781. (b) Faxén, K.; Gilderson, G.; Ädelroth, P.; Brzezinski, P. *Nature* **2005**, *437*, 286−289. (c) Schäfer, L. V.; Groenhof, G.; Klingen, A. R.; Ullmann, G. L.; Boggio-Pasqua, M.; Robb, M. A.; Grubmüller, H. *Angew. Chem., Int. Ed.* **2007**, *46*, 530−536.
(14) (a) Royant, A.; Edman, K.; Ursby, T.; Pebay-Peyroula, E.; Landau, E. M.; Neutze, R. *Nature* **2000**, *406*, 645−648. (b) Mathias, G.; Marx, D. *Proc. Natl. Acad. Sci. U.S.A.* **2007**, *104*, 6980−6985.
(15) Kwon, O.-H.; Lee, Y.-S.; Park, H. J.; Kim, Y.; Jang, D.-J. *Angew. Chem., Int. Ed.* **2004**, *43*, 5792−5796.
(16) (a) Kohtani, S.; Tagami, A.; Nakagaki, R. *Chem. Phys. Lett.* **2000**, *316*, 88−93. (b) Park, H.-J.; Kwon, O.-H.; Ah, C. S.; Jang, D.-J. *J. Chem. Phys. B* **2005**, *109*, 3938−3943. (c) Kwon, O.-H.; Lee, Y.-S.; Yoo, B. K.; Jang, D.-J. *Angew. Chem., Int. Ed.* **2006**, *45*, 415−419. (d) Park, S.-Y.; Lee, Y.-S.; Kwon, O.-H.; Jang, D.-J. *Chem. Commun.* **2009**, 926−928. (e) Park, S.-Y.; Jang, D.-J. *J. Am. Chem. Soc.* **2010**, *132*, 297−302.
(17) Smirnov, A. V.; English, D. S.; Rich, R. L.; Lane, J.; Teyton, L.; Schwabacher, A. W.; Luo, S.; Thornburg, R. W.; Petrich, J. W. *J. Chem. Phys. B* **1997**, *101*, 2758−2769.
(18) Basarić, N.; Wan, P. *Photochem. Photobiol. Sci.* **2006**, *5*, 656−664. (b) Behin Aein, N.; Wan, P. *J. Photochem. Photobiol. A: Chem.* **2009**, *208*, 42−49. (c) Basarić, N.; Cindro, N.; Hou, Y.; Žabčić, I.; Mlinarić-Majerski, K.; Wan, P. *Can. J. Chem.* **2011**, *89*, 221−234.
(19) Wirz, J. *Pure Appl. Chem.* **1998**, *70*, 2221−2232.
(20) (a) Wan, P.; Shukla, D. *Chem. Rev.* **1993**, *93*, 571−584. (b) Wan, P.; Barker, B.; Diao, L.; Fischer, M.; Shi, Y.; Yang, C. *Can. J. Chem.* **1996**, *74*, 465−475. (c) Wan, P.; Brousmiche, D. W.; Chen, C. Z.; Cole, J.; Lukeman, M.; Xu, M. *Pure Appl. Chem.* **2001**, *73*, 529−534. (d) Lukeman, M.; Wan, P. In *Handbook of organic photochemistry and photobiology*, 2nd ed.; Horspool, W., Lenci, F., Eds.; CRC Press: Boca Raton, FL, 2004; ch. 39, pp. 1−19.
(21) (a) Lukeman, M.; Wan, P. *Chem. Commun.* **2001**, 1004−1005. (b) Lukeman, M.; Wan, P. *J. Am. Chem. Soc.* **2002**, *124*, 9458−9464.
(22) Lukeman, M.; Wan, P. *J. Am. Chem. Soc.* **2003**, *125*, 1164−1165.
(23) (a) Flegel, M.; Lukeman, M.; Huck, L.; Wan, P. *J. Am. Chem. Soc.* **2004**, *126*, 7890−7897. (b) Basarić, N.; Wan, P. *J. Org. Chem.* **2006**, *71*, 2677−2686. (c) Wang, Y.-H.; Wan, P. *Photochem. Photobiol. Sci.* **2011**, *10*, 1934−1944.
(24) Nayak, M. K.; Wan, P. *Photochem. Photobiol. Sci.* **2008**, *7*, 1544−1554.
(25) Lukeman, M.; Burns, M.-D.; Wan, P. *Can. J. Chem.* **2011**, *89*, 433−440.
(26) Basarić, N.; Došlić, N.; Ivković, J.; Wang, Y.-H.; Mališ, M.; Wan, P. *Chem.—Eur. J.* **2012**, *18*, 10617−10623.
(27) Lukeman, M. PhD Disertation, University of Victoria, Victoria BC, Canada.
(28) (a) Henderson, W. A., Jr.; Zweig, A. *Tetrahedron Lett.* **1969**, *10*, 625−626. (b) Wang, C.; Piel, I.; Glorius, F. *J. Am. Chem. Soc.* **2009**, *131*, 4194−4195.
(29) Willis, M. C.; Taylor, D.; Gillmore, A. T. *Org. Lett.* **2004**, *6*, 4755−4757.
(30) Shizuka., H.; Tobita, S. *J. Am. Chem. Soc.* **1982**, *104*, 6919−6921.
(31) Webb, S. P.; Philips, L. A.; Yeh, S. W.; Tolbert, L. M.; Clark, J. H. *J. Phys. Chem.* **1986**, *90*, 5154−5164.
(32) Lukeman, M.; Veale, D.; Wan, P.; Munasinghe, R. N.; Corrie, J. E. T. *Can. J. Chem.* **2004**, *82*, 240−253.
(33) Kuhn, H. J.; Braslavsky, S. E.; Schmidt, R. *Pure Appl. Chem.* **2004**, *76*, 2105−2146.
(34) Platt, J. R. *J. Chem. Phys.* **1949**, *17*, 484−495.
(35) Pines, E., In *Chemistry of Phenols*, Ed. Rappoport, Z., John Wiley and Sons, Chichester, 2003, pp 491−528.
(36) Montalti, M.; Credi, A.; Prodi, L.; Gandolfi, M. T., In *Handbook of Photochemistry*; CRC Taylor and Francis: Boca Raton, 2006.
(37) (a) Fisher, M.; Wan, P. *J. Am. Chem. Soc.* **1999**, *121*, 4555−4562. (b) Tolbert, L. M.; Solntsev, K. M. *Acc. Chem. Res.* **2002**, *35*, 19−27. (c) Agmon, N. *J. Phys. Chem. A* **2005**, *109*, 13−35.
(38) (a) Dixon, W. T.; Murphy, D. *J. Chem. Soc., Faraday Trans. 2* **1976**, *72*, 1221−1230. (b) Levin, P. R.; Khudyakov, I. V.; Kuz'min, V. A.; Hageman, H. J.; de Jonge, C. R. H. I. *J. Chem. Soc., Perkin Trans. I* **1981**, 1237−1239. (c) Brodwell, F. G.; Cheng, J.-P. *J. Am. Chem. Soc.* **1991**, *113*, 1736−1743. (d) Gadosy, T. A.; Shukla, D.; Johnston, L. J. *J. Phys. Chem. A* **1999**, *103*, 8834−8839. (e) Shukla, D.; Schepp, N. P.; Mathivanan, N.; Johnston, L. J. *Can. J. Chem.* **1997**, *75*, 1820−1829.
(39) (a) Jacobs, H. J.; Havinga, E. *Adv. Photochem.* **1979**, *11*, 305−373. (b) Mazzucato, U.; Momicchioli, F. *Chem. Rev.* **1991**, *91*, 1679−1719.
(40) (a) Johnson, P. S.; Waters, W. A. *J. Chem. Soc.* **1962**, 4652−4655. (b) Schneider, S.; Bannwarth, W. *Angew. Chem., Int. Ed.* **2000**, *39*, 4142−4145. (c) Deng, Y.; Gong, L.; Mi, A.; Liu, H.; Jiang, Y. *Synthesis* **2003**, 337−339.
(41) (a) Howell, W. N.; Robertson, A. *J. Chem. Soc.* **1936**, 587−589. (b) Bergmann, F.; Szmuszkowicz, J.; Fawaz, G. *J. Am. Chem. Soc.* **1947**, *69*, 1773−1777. (c) Marshall, B. A.; Waters, W. A. *J. Chem. Soc.* **1959**, 381−384. (d) Baddar, F. G.; El-Assal, L. S.; Doss, N. A. *J. Chem. Soc.* **1959**, 1027−1032. (e) Roth, G. P.; Fuller, C. E. *J. Org. Chem.* **1991**, *56*, 3493−3496.
(42) (a) Repinskaya, I. B.; Abramov, A. D.; Kuklina, N. A.; Koptyug, V. A. *Zhur. Org. Khim.* **1979**, *15*, 2178−2188. (b) Denmark, S. E.; Wu, Z. *Org. Lett.* **1999**, *1*, 1495−1498. (c) Dupuis, C.; Adiey, K.; Charruault, L.; Michelet, V.; Savignac, M.; Genet, J.-P. *Tetrahedron Lett.* **2001**, *42*, 6523−6526.
(43) (a) Baddar, F. G.; El Assal, L. S. *J. Chem. Soc.* **1951**, 1844−1847. (b) Robins, P. A.; Walker, J. *J. Chem. Soc.* **1958**, 409−421.
(44) (a) Luttringhaus, A.; Saaf, G. W. *Justus Liebigs Ann. Chem.* **1945**, *557*, 25−45. (b) Friedel, R. A.; Orchin, M.; Reggel, L. *J. Am. Chem. Soc.* **1948**, *70*, 199−204. (c) Ohe, K.; Yokoi, T.; Miki, K.; Nishino, F.; Uemura, S. *J. Am. Chem. Soc.* **2002**, *124*, 526−527.
(45) (a) Hodgson, H. H.; Foster, C. K. *J. Chem. Soc.* **1942**, 581−583. (b) Bumagin, N. A.; Tsarev, D. A. *Tetrahedron Lett.* **1998**, *39*, 8155−8188.
(46) Borsche, W.; Kettner, S.; Gilles, M.; Kuhn, H.; Manteuffel, R. *Justus Liebigs Ann. Chem.* **1936**, *526*, 1−22. (b) Kruber, O.; Raeithel, A. *Chem. Ber.* **1953**, *86*, 366−371. (c) Wawzonek, S.; Kozikowski, J. *J. Am. Chem. Soc.* **1954**, *76*, 1641−1643.
(47) (a) Ishii, H.; Hanaoka, T.; Ikeda, N. *Yakugaku Zasshi* **1976**, *96*, 1161−1168. (b) Ishii, H.; Hanaoka, T.; Asaka, T.; Harada, Y.; Ikeda, N. *Tetrahedron* **1976**, *32*, 2693−2698.
(48) Eichkorn, K.; Treutler, O.; Öhm, H.; Häser, M.; Ahlrichs, R. *Chem. Phys. Lett.* **1995**, *242*, 652−660.
(49) Tomasi, J.; Mennucci, B.; Cammi, R. *Chem. Rev.* **2005**, *105*, 2999−3094.
(50) Frisch, M. J.; Trucks, G. W.; Schlegel, H. B.; Scuseria, G. E.; Robb, M. A.; Cheeseman, J. R.; Montgomery, Jr., J. A.; Vreven, T.; Kudin, K. N.; Burant, J. C.; Millam, J. M.; Iyengar, S. S.; Tomasi, J.; Barone, V.; Mennucci, B.; Cossi, M.; Scalmani, G.; Rega, N.; Petersson, G. A.; Nakatsuji, H.; Hada, M.; Ehara, M.; Toyota, K.; Fukuda, R.; Hasegawa, J.; Ishida, M.; Nakajima, T.; Honda, Y.; Kitao, O.; Nakai, H.; Klene, M.; Li, X.; Knox, J. E.; Hratchian, H. P.; Cross, J. B.; Adamo, C.; Jaramillo, J.; Gomperts, R.; Stratmann, R. E.; Yazyev, O.; Austin, A. J.; Cammi, R.; Pomelli, C.; Ochterski, J. W.; Ayala, P. Y.; Morokuma, K.; Voth, G. A.; Salvador, P.; Dannenberg, J. J.; Zakrzewski, V. G.; Dapprich, S.; Daniels, A. D.; Strain, M. C.; Farkas, O.; Malick, D. K.; Rabuck, A. D.; Raghavachari, K.; Foresman,

J. B.; Ortiz, J. V.; Cui, Q.; Baboul, A. G.; Clifford, S.; Cioslowski, J.; Stefanov, B. B.; Liu, G.; Liashenko, A.; Piskorz, P.; Komaromi, I.; Martin, R. L.; Fox, D. J.; Keith, T.; Al-Laham, M. A.; Peng, C. Y.; Nanayakkara, A.; Challacombe, M.; Gill, P. M. W.; Johnson, B.; Chen, W.; Wong, M. W.; Gonzalez, C.; Pople, J. A. *Gaussian 03*, Rev E.01; Gaussian, Inc.: Pittsburgh PA, 2003.

(51) Christiansen, O.; Koch, H.; Jorgensen, P. *Chem. Phys. Lett.* **1995**, *243*, 409−418.

(52) Weigend, F.; Häser, M. *Theor. Chem. Acc.* **1997**, *97*, 331−340.

(53) Foster, J. P.; Weinhold, F. *J. Am. Chem. Soc.* **1980**, *102*, 7211−7218.

(54) Ahlrichs, R.; Bär, M.; Häser, M.; Horn, H.; Kölmel, C. *Chem. Phys. Lett.* **1989**, *162*, 165−169.